J|A|C|S
ARTICLES
Published on Web 09/02/2005

NMR Spectroscopic Characterization of Millisecond Protein Folding by Transverse Relaxation Dispersion Measurements

Markus Zeeb† and Jochen Balbach*,‡

Contribution from the Laboratorium für Biochemie, Universität Bayreuth, D-95440 Bayreuth, Germany

Received February 22, 2005; E-mail: jochen.balbach@physik.uni-halle.de

Abstract: The cold shock protein CspB adopts its native and functional tertiary structure on the millisecond time scale. We employed transverse relaxation NMR methods, which allow a quantitative measurement of the cooperativity of this fast folding reaction on a residue basis. Thereby, chemical exchange contributions to the transverse relaxation rate (R_2) were observed for every residue of CspB verifying the potential of this method to identify not only local dynamics but also to characterize global events. Toward this end, the homogeneity of the transition state of folding was probed by comparing Chevron plots (i.e., dependence of the apparent folding rate on the denaturant concentration) determined by stopped-flow fluorescence with Chevron plots of six residues acquired by R_2 dispersion experiments. The coinciding results obtained for probes at different locations in the three-dimensional structure of CspB indicate the ability and significance of transverse relaxation NMR to determine Chevron plots on a residue-by-residue basis providing detailed insights on the nature of the transition state of folding.

Introduction

Protein folding is one of the most relevant topics in structural biology and the mechanism by which proteins adopt their native and functional tertiary conformation is still widely discussed. Time constants of protein folding reactions range between microseconds and days. In the past decade, many extremely fast folding proteins were characterized in detail.[1−9] The characterization of these fast reactions with conventional stopped-flow mixing devices require experimental finesse. Therefore, dynamic NMR methods such as extended Lipari-Szabo analyses of ^{15}N relaxation data,[10] ^{15}N $R_1\rho$ measurements,[7] or ^{1}H line shape analyses[1,6,9,11] are key methods in the determination of such high folding rates since the rapid conversion of exchanging states under equilibrium conditions can be exploited. The ^{1}H line shape analysis was successfully applied to a system which achieves its native conformation in a few microseconds.[9] A disadvantage of the latter approach is that over a wide range of conditions, a well-resolved unperturbed resonance is required. In addition, the sensitivity of this method drops dramatically if both exchanging states are not significantly populated simultaneously, which limits experimental conditions significantly.

In this article, we describe the application of ^{15}N transverse relaxation dispersion curves[12−19] ($R_2(1/\tau_{cp})$) to study millisecond protein folding at a residue level, which overcomes both previously raised limitations. Chemical or conformational exchange (R_{ex}) on the microsecond-to-millisecond time scale contributes significantly to R_2 even at very small populations of one exchanging state[15] and the use of 2D ^{1}H−^{15}N correlation spectra alleviates resonance overlap. Therefore, R_2 dispersion measurements are well suited to characterize not only local but also global folding reactions even under strongly native conditions, where only a small fraction of the unfolded state is present.

R_2 dispersion was applied to the small 67 amino acid containing cold shock protein CspB from *Bacillus* subtilis, which

† Current address: Department of Molecular Biology, The Scripps Research Institute, La Jolla, CA 92037, USA.
‡ Current address: Fachgruppe Biophysik, Martin-Luther-Universität Halle-Wittenberg, D-06099 Halle (Saale), Germany.

(1) Huang, G. S.; Oas, T. G. *Proc. Natl. Acad. Sci. U.S.A.* **1995**, *92*, 6878−6882.
(2) Schindler, T.; Herrler, M.; Marahiel, M. A.; Schmid, F. X. *Nat. Struct. Biol.* **1995**, *2*, 663−673.
(3) Burton, R. E.; Huang, G. S.; Daugherty, M. A.; Fullbright, P. W.; Oas, T. G. *J. Mol. Biol.* **1996**, *263*, 311−322.
(4) Kragelund, B. B.; Hojrup, P.; Jensen, M. S.; Schjerling, C. K.; Juul, E.; Knudsen, J.; Poulsen, F. M. *J. Mol. Biol.* **1996**, *256*, 187−200.
(5) Kuhlman, B.; Boice, J. A.; Fairman, R.; Raleigh, D. P. *Biochemistry* **1998**, *37*, 1025−1032.
(6) Spector, S.; Raleigh, D. P. *J. Mol. Biol.* **1999**, *293*, 763−768.
(7) Vugmeyster, L.; Kroenke, C. D.; Picart, F.; Palmer, A. G., 3rd; Raleigh, D. P. *J. Am. Chem. Soc.* **2000**, *122*, 5387−5388.
(8) Myers, J. K.; Oas, T. G. *Nat. Struct. Biol.* **2001**, *8*, 552−558.
(9) Wang, M.; Tang, Y.; Sato, S.; Vugmeyster, L.; McKnight, C. J.; Raleigh, D. P. *J. Am. Chem. Soc.* **2003**, *125*, 6032−6033.
(10) Zeeb, M.; Jacob, M. H.; Schindler, T.; Balbach, J. *J. Biomol. NMR* **2003**, *27*, 221−234.
(11) Zeeb, M.; Balbach, J. *Protein Peptide Lett.* **2005**, *12*, 139−146.
(12) Loria, J. P.; Rance, M.; Palmer, A. G., 3rd *J. Am. Chem. Soc.* **1999**, *121*, 2331−2332.
(13) Tollinger, M.; Skrynnikov, N. R.; Mulder, F. A.; Forman-Kay, J. D.; Kay, L. E. *J. Am. Chem. Soc.* **2001**, *123*, 11341−11352.
(14) Palmer, A. G., III; Kroenke, C. D.; Loria, J. P. *Methods Enzymol.* **2001**, *339*, 204−238.
(15) Korzhnev, D. M.; Salvatella, X.; Vendruscolo, M.; Di Nardo, A. A.; Davidson, A. R.; Dobson, C. M.; Kay, L. E. *Nature* **2004**, *430*, 586−590.
(16) Korzhnev, D. M.; Kloiber, K.; Kay, L. E. *J. Am. Chem. Soc.* **2004**, *126*, 7320−7329.
(17) Orekhov, V. Y.; Korzhnev, D. M.; Kay, L. E. *J. Am. Chem. Soc.* **2004**, *126*, 1886−1891.
(18) Di Nardo, A. A.; Korzhnev, D. M.; Stogios, P. J.; Zarrine-Afsar, A.; Kay, L. E.; Davidson, A. R. *Proc. Natl. Acad. Sci. U.S.A.* **2004**, *101*, 7954−7959.
(19) Choy, W. Y.; Zhou, Z.; Bai, Y. W.; Kay, L. E. *J. Am. Chem. Soc.* **2005**, *127*, 5066−5072.

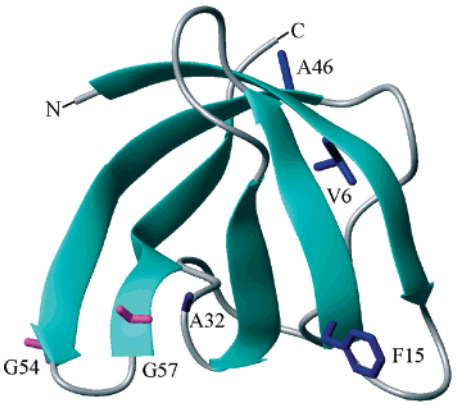

Figure 1. Ribbon drawing of the cold-shock protein CspB from *Bacillus subtilis*. The MOLMOL[40] representation is based on the coordinates from the protein data bank file 1csp.pdb[28] and depicts residues Val6, Phe15, Ala32, Ala46, Gly54, and Gly57, which backbone ^{15}N R_2 dispersion has been used to determine un- and refolding rates on a millisecond time scale. Gly54 and Gly57 (magenta) are represented by the bonds between Cα and Hα whereas for Val6, Phe15, Ala32, and Ala46 (blue) the bonds between the side chain heavy atoms are shown.

served as a model protein in numerous protein folding studies.[2,11,20−27] The structure of CspB (Figure 1) comprises a five stranded antiparallel β-sheet forming an OB-folded β-barrel.[28,29] Its native structure is obtained via a simple two-state folding mechanism and CspB was one of the first described examples of millisecond protein folding.[2] Stopped-flow fluorescence experiments revealed extrapolated folding and unfolding rates in the absence of denaturant ($k_f^{H_2O}$ and $k_u^{H_2O}$) of 1070 ± 20 s^{-1} and of 12 ± 7 s^{-1}, respectively. These millisecond rates of global folding could be verified by their R_{ex} contribution to R_2 from extended Lipari−Szabo analyses of ^{15}N NMR relaxation data under native conditions as well as from ^1H-^{15}N dipolar/^{15}N chemical shift anisotropy relaxation interference experiments.[10] In the present study, we employed R_2 dispersion experiments to determine k_f and k_u under various urea concentrations. The analysis of the urea concentration dependence of folding rates is a standard procedure in protein folding studies to determine the solvent accessibility of the transition state (TS) of folding and to kinetically characterize folding and unfolding intermediates.[30] Typically, stopped-flow fluorescence or stopped-flow circular dichroism spectroscopy is exploited to gain folding rates from local fluorescent reporters or secondary structure elements, respectively. The here presented NMR study demonstrates that the urea dependence of k_f and k_u could be determined on a residue-by-residue basis with R_2 dispersion measurements allowing the characterization of the homogeneity of the transition state of protein folding.

Materials and Methods

Sample Preparation. The cold shock protein CspB from *Bacillus subtilis* was expressed in *E. coli* BL21(DE3) pPDCSP as described previously.[10] Uniformly ^{15}N isotope enrichment was achieved by growing the bacteria in M9 minimal media,[31] which was supplemented with ^{15}N ammonium chloride as sole nitrogen source. The purification of the protein was performed as described before.[2] All NMR samples for R_2 dispersion measurements contained 1.5 mM uniformly ^{15}N labeled CspB in 20 mM Na-cacodylate/HCl pH 7.0 in $H_2O/^2H_2O$ (90%/10%) in the absence or presence of 1.2, 2.0, 3.1, 4.2, 5.3, or 6.4 M urea, respectively. 2D ZZ exchange spectra were acquired with NMR samples of 1 mM ^{15}N labeled CspB in the presence of 2.7, 3.0, 3.3, 3.5, 3.9, 4.2, and 4.7 M urea.

NMR Spectroscopy. All experiments were recorded at 25 °C on Bruker Avance spectrometers at ^1H resonance frequencies of 500, 600, 700, and 750 MHz. Relaxation compensated Carr−Purcell−Meiboom−Gill (CPMG) pulse sequences published by Palmer and co-workers[12,32] were used to record dispersion curves of the transverse relaxation rate R_2. Briefly, chemical exchange (R_{ex}) on the microsecond-to-millisecond time scale contributes significantly to R_2 ($R_2 = R_2° + R_{ex}$). This contribution of R_{ex} to R_2 can be modulated by the variation of the delay τ_{cp}, which represents the time between consecutive ^{15}N 180° pulses in the spin−echo CPMG pulse sequence. R_2 was determined by the decay of cross-peak intensities using 5 to 8 different relaxation delays between 2.6 ms and 208 ms with a fixed spin−echo delay τ_{cp}. In case of less than 5 applicable relaxation delays due to rapid intensity decay (i.e., for long τ_{cp} values), multiple spectra with 3 or 4 different relaxation delays were acquired. Uncertainties in cross-peak intensities were estimated by duplicate recorded spectra of two relaxation delays. Dispersion curves were generated by evaluating R_2 rates for 8 to 10 different τ_{cp} values between 650 μs and 21.6 ms. Spectra were acquired with (2048 × 96) complex points and 16 transients for each complex point using spectral widths of 11218 Hz (^1H) and 2058 Hz (^{15}N) at 16.4 T, 9615 Hz (^1H) and 1764 Hz (^{15}N) at 14.1 T or, 8013 Hz (^1H) and 1470 Hz (^{15}N) at 11.7 T, respectively. R_2 dispersion curves were recorded in the presence of 0 or 3.1 M urea at 16.4 T and of 1.2, 2.0, 3.1, 4.2, 5.3, and 6.4 M urea at 14.1 T, as well as of 2.0 M urea at 11.7 T, respectively.

For the assignment of cross-peaks of unfolded CspB 2D $^1H-^{15}N$ ZZ-exchange spectra[33−35] were recorded at 750 MHz in the presence of 2.7 to 4.7 M urea. Under these conditions, the native and unfolded state of CspB undergoes slow chemical exchange in respect to the NMR chemical shift time scale ($k_{ex} < \Delta\omega$) and therefore shows distinct cross-peaks for each state in the 2D ZZ exchange spectrum. To transfer the assignments of the cross-peaks of the native state under native conditions to the presence of 2.7 M urea a series of $^1H-^{15}N$ HSQC spectra with increasing urea concentration was recorded. The cross-peaks of the unfolded state could be assigned by correlating the cross-peaks of the native state with the two exchange cross-peaks. The latter were identified by varying the exchange time between 1 ms and 150 ms, which modulates cross-peak intensities of the auto (native or unfolded CspB) and exchange cross-peaks contrarily. To validate the assignments, two ZZ exchange spectra with a mixing time of 60 ms were recorded in which the exchange delay was located either prior or after the evolution of ^{15}N chemical shift.[34] The subtraction of these

(20) Schindler, T.; Schmid, F. X. *Biochemistry* **1996**, *35*, 16833−16842.
(21) Jacob, M.; Schindler, T.; Balbach, J.; Schmid, F. X. *Proc. Natl. Acad. Sci. U.S.A.* **1997**, *94*, 5622−5627.
(22) Perl, D.; Welker, C.; Schindler, T.; Schröder, K.; Marahiel, M. A.; Jaenicke, R.; Schmid, F. X. *Nat. Struct. Biol.* **1998**, *5*, 229−235.
(23) Jacob, M.; Geeves, M.; Holtermann, G.; Schmid, F. X. *Nat. Struct. Biol.* **1999**, *6*, 923−926.
(24) Jacob, M.; Holtermann, G.; Perl, D.; Reinstein, J.; Schindler, T.; Geeves, M. A.; Schmid, F. X. *Biochemistry* **1999**, *38*, 2882−2891.
(25) Jacob, M.; Schmid, F. X. *Biochemistry* **1999**, *38*, 13773−13779.
(26) Jacob, M. H.; Saudan, C.; Holtermann, G.; Martin, A.; Perl, D.; Merbach, A. E.; Schmid, F. X. *J. Mol. Biol.* **2002**, *318*, 837−845.
(27) Garcia-Mira, M. M.; Boehringer, D.; Schmid, F. X. *J. Mol. Biol.* **2004**, *339*, 555−569.
(28) Schindelin, H.; Marahiel, M. A.; Heinemann, U. *Nature* **1993**, *364*, 164−168.
(29) Schnuchel, A.; Wiltschek, R.; Czisch, M.; Herrler, M.; Willimsky, G.; Graumann, P.; Marahiel, M. A.; Holak, T. A. *Nature* **1993**, *364*, 169−171.
(30) Bachmann, A.; Kiefhaber, T. In *Protein Folding Handbook*; Buchner, J., Kiefhaber, T., Eds.; Wiley-VCH: Weinheim, 2005; pp 379−406.
(31) Sambrook, J.; Fritsch, E. F.; Maniatis, T. 1989 *Molecular Cloning: A Laboratory Manual*; Cold Spring Harbor Laboratory Press: Cold Spring Harbor, New York.
(32) Millet, O.; Loria, J. P.; Kroenke, C. D.; Pons, M.; Palmer, A. G., 3rd *J. Am. Chem. Soc.* **2000**, *122*, 2867−2877.
(33) Montelione, G. T.; Wagner, G. *J. Am. Chem. Soc.* **1989**, *111*, 3096−3098.
(34) Wider, G.; Neri, D.; Wüthrich, K. *J. Biomol. NMR* **1991**, *1*, 93−98.
(35) Farrow, N. A.; Zhang, O.; Forman-Kay, J. D.; Kay, L. E. *J. Biomol. NMR* **1994**, *4*, 727−734.

two spectra revealed positive or negative intensities for the auto or exchange cross-peaks, respectively, which allowed a straightforward assignment of auto and exchange cross-peaks. In addition, the assignment of the unfolded state enabled us to determine the chemical shift differences between cross-peaks of the native and unfolded protein ($\Delta\delta_{NU}$ in ppm). The urea dependence of $\Delta\delta_{NU}$ was elucidated by ZZ exchange experiments at 7 different urea concentrations between 2.7 and 4.7 M. Linear extrapolation was used to obtain $\Delta\delta_{NU}$ over the entire urea concentration range of the R_2 dispersion measurements. Populations of the native and unfolded state were calculated by the respective auto cross-peak intensities of the two exchanging states in the 2D ZZ exchange or $^1H-^{15}N$ HSQC spectra at the respective urea concentration ($p_N = I_N/(I_N + I_U)$, $p_U = 1 - p_N$). These results correlate very well to independently determined populations by fluorescence detected stopped-flow or equilibrium experiments.[2] Processing and analysis of all spectra was carried out with Felix97 (MSI).

Data Analysis. Determination of R_2 was performed by fitting a simple exponential function without offset to the data ($I = A\cdot\exp(-R_2\cdot t)$) using Grafit (Erithacus software). R_2 values are plotted versus $1/\tau_{cp}$ to obtain R_2 dispersion curves. The latter were analyzed with the program CPMGfit (kindly provided by A. G. Palmer, Columbia University) or Scientist (Micromath) using the general expression for $R_2(1/\tau_{cp})$ (eq 1), which is independent of the exchange regime (slow, intermediate or fast exchange in respect to the NMR chemical shift time scale) because no assumptions about the exchange regime were applied to derive eq 1. Moreover, eq 1 is independent of the equilibrium population ratio of the two exchanging states[32] and therefore valid under all studied conditions. It is given by[14,32,36]

$$R_2(1/\tau_{cp}) = \frac{1}{2}\left(R_{2N} + R_{2U} + k_{ex} - \frac{1}{\tau_{cp}}\cosh^{-1}[D_+\cosh(\eta_+) - D_-\cosh(\eta_-)]\right) \quad (1)$$

with

$$D_\pm = \frac{1}{2}\left[\pm 1 + \frac{\psi + 2\Delta\omega^2}{\sqrt{\psi^2 + \zeta^2}}\right]$$

$$\eta_\pm = \frac{\tau_{cp}}{\sqrt{2}}\sqrt{\pm\psi + \sqrt{\psi^2 + \zeta^2}}$$

$$\psi = (R_{2N} - R_{2U} - p_N k_{ex} + p_U k_{ex})^2 - \Delta\omega^2 + 4p_N p_U {k_{ex}}^2$$

$$\zeta = 2\Delta\omega\cdot(R_{2N} - R_{2U} - p_N k_{ex} + p_U k_{ex})$$

where R_{2N} and R_{2U} are the ^{15}N transverse relaxation rates of the native and unfolded state in the absence of chemical exchange, p_N and p_U are the equilibrium populations of the respective state, k_{ex} is the exchange rate between the two states ($k_{ex} = k_f + k_u$), k_f and k_u are the folding and unfolding rate constant, and $\Delta\omega$ is the difference of the ^{15}N chemical shift between the cross-peak of the respective backbone amide in the native and the unfolded conformation ($\Delta\omega = 2\pi\cdot\Delta\delta_{NU}\cdot\omega_N$ with ω_N as the ^{15}N resonance frequency and $\Delta\delta_{NU}$ as the difference in chemical shift between the native and unfolded state in ppm).

The determination of k_{ex} at every urea concentration was achieved by fitting eq 1 to the R_2 dispersion curve using fixed populations (p_N, p_U) and fixed chemical shift differences ($\Delta\omega$). $\Delta\omega$ was independently obtained from the 2D ZZ exchange experiments, whereas the populations were extracted from stopped-flow fluorescence measurements.[2] As mentioned above, the latter results correspond to populations accomplished from cross-peak intensities of the 2D ZZ exchange experiments or from intensities of the respective cross-peaks in a $^1H-^{15}N$ HSQC detected urea induced unfolding transition of CspB. At urea concentrations between 0 and 4.2 M intensities of cross-peaks of the native protein were analyzed to obtain R_2. Evaluation of k_{ex} was carried out with fixed R_{2U} values which were linearly extrapolated from their urea dependence between 5.3 and 6.4 M urea. In the latter urea concentration region, cross-peak intensities of the unfolded proteins were used to determine R_2 and R_2 dispersion curves were fitted using fixed R_{2N} values according to their urea dependence between 0 and 4.2 M urea. The accuracy of the fitting procedure with fixed p_N, p_U, and $\Delta\omega$ was confirmed by simultaneous fitting of R_2 dispersion curves at two static magnetic field strengths in the presence of 2.0 or 3.1 M urea (11.7 and 14.1 T or 14.1 and 16.4 T, respectively), which revealed identical results for p_N, p_U, and k_{ex}.

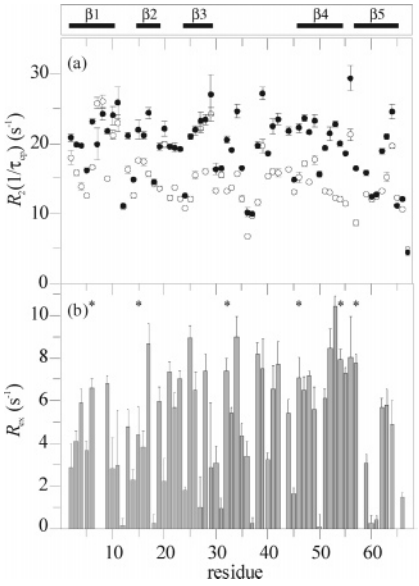

Figure 2. Dynamic folding equilibrium of CspB causes a τ_{cp} dependence of R_2 for each residue. (a) $R_2(1/\tau_{cp})$ of CspB for τ_{cp} =1 ms (open circles) and τ_{cp} = 10 ms (filled circles), respectively, are plotted versus the residue number. Spectra were recorded on a 1.5 mM ^{15}N enriched CspB sample in 20 mM Na-cacodylate/HCl pH 7.0 at B_0 = 14.1 T and 25 °C with a Bruker Avance600 in the presence of 1.2 M urea. (b) Chemical exchange contribution R_{ex} to R_2 as estimated by the difference of the transverse relaxation rates depicted in (a): $R_{ex} = R_2(1/10\text{ ms}) - R_2(1/1\text{ ms})$. Asterisks specify residues whose Chevron plots (urea dependence of the exchange rate k_{ex}) are shown in Figure 6. The black bars at the top indicate residues, which form the five β-strands of the β-barrel structure of CspB.

Results and Discussion

Determination of R_{ex} and $\Delta\omega$. Chemical exchange contributions to transverse relaxation rates are used to identify local[12,37,38] and global[13−19,32] dynamics on the microsecond-to-millisecond time scale. Local dynamics are frequently present in flexible loop regions of proteins or occur in the neighborhood of isomerizing disulfide bonds. Global dynamics on this time scale can result from the equilibrium conversion between the native state and the fully unfolded polypeptide chain.

For the cold shock protein CspB, we found global R_{ex} contributions to R_2 ($R_2 = R_2^0 + R_{ex}$) evenly distributed over each residue of the protein (Figure 2). In Figure 2a, $R_2(1/\tau_{cp})$ is plotted for a spin−echo delay τ_{cp} of 1 ms and 10 ms. For the short spin−echo delay R_2^0 dominates R_2, whereas for the long spin−echo delay additional R_{ex} contributions are detectable. The difference of both data sets is depicted in Figure 2b to estimate

(36) Carver, J. P.; Richards, R. E. *J. Magn. Reson.* **1972**, *6*, 89−105.
(37) Mulder, F. A.; Mittermaier, A.; Hon, B.; Dahlquist, F. W.; Kay, L. E. *Nat. Struct. Biol.* **2001**, *8*, 932−935.
(38) Mulder, F. A.; Hon, B.; Mittermaier, A.; Dahlquist, F. W.; Kay, L. E. *J. Am. Chem. Soc.* **2002**, *124*, 1443−1451.

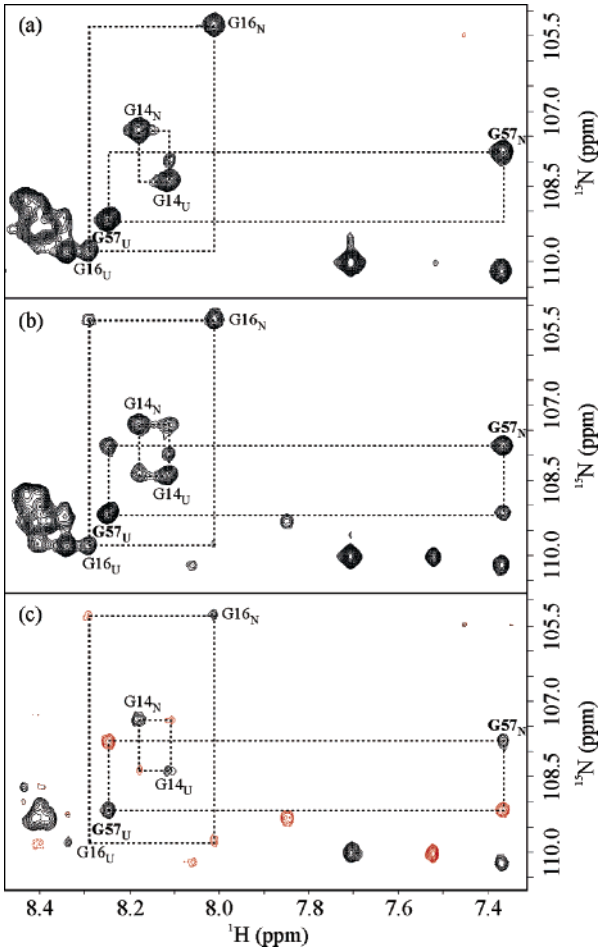

Figure 3. Section of 2D ^{15}N ZZ exchange spectra of CspB at 750 MHz in 20 mM Na-cacodylate/HCl pH 7.0 at 25 °C in the presence of 3.1 M urea and an exchange delay of 60 ms. (a) The reference spectrum contains solely cross-peaks of the native and the unfolded state (auto cross-peaks). (b) The ZZ exchange spectrum shows auto cross-peaks with reduced intensity as well as additional exchange cross-peaks. (c) The difference spectrum of the reference and the exchange spectrum (a−b) yields residual positive intensities for the auto cross-peaks (solid black line) and negative intensities for the exchange cross-peaks (solid red line). The assignment of cross-peaks is given in the spectra. Dashed lines connect auto and exchange cross-peaks of one backbone amide.

R_{ex} ($R_{ex} = R_2 - R_2^0$) for each backbone amide of CspB. If we assume the same global $k_f^{H_2O}$ and $k_u^{H_2O}$ rate for each residue, then the modulation of R_{ex} results solely from the variable difference in ^{15}N chemical shifts between the unfolded and folded state ($\Delta\omega$). However, local dynamics of the polypeptide chain might contribute as well to the observed R_{ex} values.

The reliability of fitting eq 1 to R_2 dispersion curves acquired at a single magnetic field strength improves significantly if $\Delta\omega$ is known. Fortunately, at moderate urea concentrations, the folding rates of CspB are within the limits for 2D ZZ exchange spectroscopy.[33−35] The 2D ^{1}H−^{15}N correlation experiment with the delay for chemical exchange before the ^{15}N chemical shift evolution time (t_1) gives the reference spectrum where only the auto cross-peaks of the two exchanging states are present (Figure 3a). If the delay for chemical exchange is located after t_1 the 2D spectrum contains both the auto and exchange cross-peaks (Figure 3b). Subtracting the latter from the reference spectrum yields residual positive intensities for the auto cross-peaks and negative intensities for the exchange cross-peaks (Figure 3c).

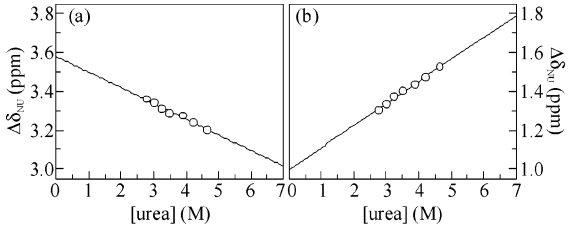

Figure 4. Urea dependence of the difference of the ^{15}N chemical shift ($\Delta\delta_{NU}$) between the cross-peak of the native and unfolded state of (a) Gly54 and (b) Gly57. $\Delta\delta_{NU}$ was extracted from 2D ^{15}N ZZ exchange spectra of CspB in 20 mM Na-cacodylate/HCl pH 7.0 at 25 °C in the presence of various urea concentrations between 2.7 and 4.7 M at 750 MHz. The solid line represents the fit of a linear equation to the data yielding a slope and an offset for Gly54 of (−0.081 ± 0.005) ppm·M^{-1} and (3.578 ± 0.019) ppm, and for Gly57 of (0.113 ± 0.004) ppm·M^{-1} and (0.996 ± 0.015) ppm, respectively.

The exchange cross-peaks allowed the direct assignment of the respective amide nuclei in the unfolded state.

Since auto and exchange cross-peaks could be observed between 2.7 and 4.7 M urea $\Delta\delta_{NU}$ was calculated as the chemical shift difference between the auto cross-peaks of the respective amide. To determine $\Delta\omega$ ($\Delta\omega = 2\pi\cdot\Delta\delta_{NU}\cdot\omega_N$) at urea concentrations, where 2D ZZ exchange spectroscopy was not sensitive enough due to too low populations of one state or too high folding rates, the experimentally derived $\Delta\delta_{NU}$ values were extrapolated assuming a linear urea dependence of $\Delta\delta_{NU}$ (Figure 4). This linearity has been also observed in an NMR detected urea induced unfolding transition where the chemical shifts of the backbone amides of the native or unfolded state could be followed down to 0 M or up to 6 M urea, respectively (data not shown). The latter was feasible because the assignment of the cross-peaks between 2.7 and 4.7 M urea was achieved by the before mentioned ZZ exchange experiments.

Global versus Local Dynamics. A not identified R_{ex} from local breathing on a microsecond-to-millisecond time scale can falsify the global rates of folding determined under the assumption of a two-state model. Therefore, the next step was to distinguish between local and global R_{ex} contributions to R_2. For this purpose, the populations of native and unfolded state in the absence of urea were altered by adding up to 70% ethylene glycol (EG) to the solution.[10] EG shifts the two-state equilibrium toward the native state and decreases both $k_f^{H_2O}$ and $k_u^{H_2O}$. This leads to a loss of observable R_{ex} contributions from global folding due to the substantially decreased population of U as well as to the decreased folding rates. At 70% EG, an extended Lipari−Szabo analysis revealed residual R_{ex} contributions below 3 Hz in the loop between β-strands 2 and 3 of CspB (Glu21-Gln23) and the extended loop region between β-strands 3 and 4 (Glu36-Thr40).[10] These R_{ex} values can be attributed to local dynamics. Consequently, six residues of CspB without observable local dynamics (Val6, Phe15, Ala32, Ala46, Gly54, Gly57) have been selected for the determination of global folding rates from R_2 dispersion experiments.

Analysis of R_2 Dispersion Curves at Various Urea Concentrations. The quantitative analysis of the two-state exchange rate between the native and unfolded state was accomplished by fitting eq 1 to the R_2 dispersion curve of representative backbone amides using independently determined differences in chemical shifts $\Delta\omega$. Populations of the native and unfolded state at respective urea concentrations, p_N and p_U, were obtained from fluorescence detected stopped-flow experiments[2] and peak

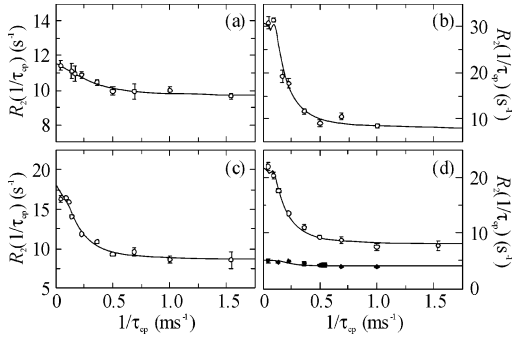

Figure 5. Relaxation dispersion curves of Gly57 of CspB. Values of R_2 as a function of $1/\tau_{cp}$ in the presence of (a) 0 M, (b) 3.1 M, (c) 1.2 M, and (d) (circles) 2.0 M, (filled diamonds) 6.4 M urea are depicted. Data were acquired at $B_0 = 14.1$ T (60.84 MHz ^{15}N frequency) except for the data at 0 and 3.1 M urea, which were recorded at $B_0 = 16.4$ T (70.98 MHz ^{15}N frequency). The solid lines represent fits of eq 1 to the data using fixed differences in ^{15}N chemical shift between the native and unfolded conformation ($\Delta\omega$) as well as fixed populations of the native state (p_N). $\Delta\omega$ was determined by 2D ZZ spectroscopy in the presence of 2.7 to 4.7 M urea and linearly extrapolated to the absence of denaturant (70.7, 69.1, 74.4, 95.6, and 104.7 Hz for 0, 1.2, 2.0, 3.1, and 6.4 M urea, respectively). p_N was obtained by stopped-flow fluorescence experiments (0.992, 0.957, 0.894, 0.734, and 0.063 for 0, 1.2, 2.0, 3.1, and 6.4 M urea, respectively) and verified by a urea induced unfolding transition monitored by ^{1}H$-^{15}$N HSQC spectra. It revealed $k_{ex} = k_f + k_u$ rates of 903 ± 200 s^{-1} at 0 M, 357 ± 94 s^{-1} at 1.2 M, 137 ± 7 s^{-1} at 2.0 M, 93 ± 6 s^{-1} at 3.1 M, and 27 ± 4 s^{-1} at 6.4 M urea, respectively, also depicted in Figure 6f. It is noteworthy that the data in the presence of 5.3 and 6.4 M urea are based on cross-peak intensities of the unfolded state.

volumes of respective cross-peaks of a ^{1}H$-^{15}$N HSQC detected urea induced unfolding transition. Fitting of eq 1 to a R_2 dispersion curve at a given urea concentration acquired at a single magnetic field was performed with fixed $\Delta\omega$ and fixed populations. The latter were varied by altering the urea concentration, which affects k_{ex} and therefore the R_2 dispersion profiles.

Figure 5 depicts R_2 dispersion curves of CspB residue Gly57 at five different denaturant concentrations between 0 and 6.4 M urea covering the entire urea induced unfolding transition. The folding rates derived from these fits are shown in Figure 6f. As a verification of the fitting procedure using fixed populations, R_2 dispersion data at two magnetic field strengths were fitted simultaneously for two urea concentrations to obtain k_{ex}, p_N, and p_U. These fits revealed equal exchange rates and confirmed the otherwise determined populations (data not shown) indicating the consistency of the applied fitting procedure for data acquired at a single magnetic field strength.

A characterization of the transition state of a protein folding reaction following a two-state mechanism can be achieved by the dependence of the apparent folding rate ($k_{ex} = k_f + k_u$) of the urea concentration, which was determined by the analysis of R_2 dispersion profiles. From the slopes of the urea dependences of log k_f and log k_u, m_f and m_u, the Tanford factor $\beta^T = m_f/(m_f - m_u)$ can be calculated. For CspB, β^T is close to 0.9 when determined by stopped-flow fluorescence[2] or dynamic 1D NMR spectroscopy.[11] A β^T factor close to 1 indicates a native like transition state in terms of its solvent accessible surface area.[30] To validate the reliability of the present k_{ex} determined from R_2 dispersion curves, a comparison to previously published data employing stopped-flow fluorescence measurements[2] is illustrated in Figure 6 for six backbone amides. Open symbols represent the NMR derived apparent folding rates, whereby the solid and broken lines depict k_{ex} and the intrinsic folding rates

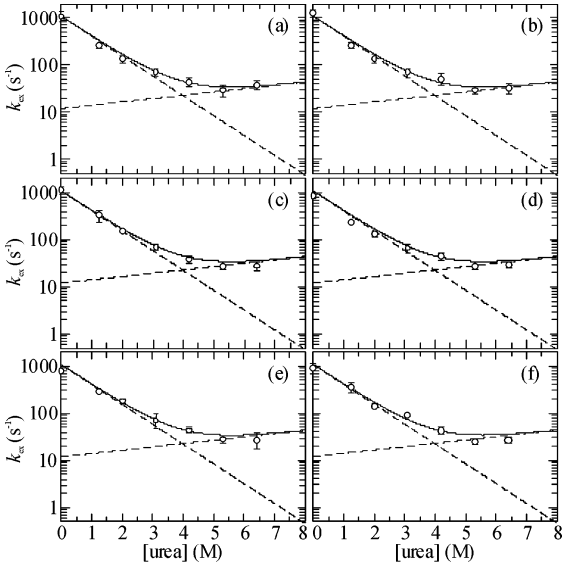

Figure 6. Chevron plot of the exchange rate versus the urea concentration of (a) Val6, (b) Phe15, (c) Ala32, (d) Ala46, (e) Gly54, and (f) Gly57 of CspB. k_{ex} at the respective urea concentration was determined using $R_2(1/\tau_{cp})$ dispersion curves as depicted in Figure 5. The solid line represents k_{ex} and the broken lines correspond to the extrapolated intrinsic refolding and unfolding rates (k_f and k_u) of the fluorescence detected stopped-flow experiments.[2] Uncertainties of k_{ex} determined by R_2 dispersion are depicted by the respective error bars.

(k_f, k_u) as a function of the urea concentration, respectively, both acquired from fluorescence detected stopped-flow data. The rates observed by both techniques are very similar and show the equivalent dependence on the urea concentration. These coinciding results of such diverse probes (Trp8 for fluorescence, Val6, Phe15, Ala32, Ala46, Gly54, Gly57 for R_2 dispersion), which are either in proximity or widely separated in sequence and in the three-dimensional structure of CspB (Figure 1), confirm the sensitivity of the fluorescent local probe for global folding events and emphasize the significance of the results obtained from R_2 dispersion experiments. This also confirms the sensitivity of Val6, Phe15, Ala32, Ala46, Gly54, and Gly57 to global folding in the absence of local dynamics.

Implications for Protein Folding. Chevron plots such as depicted in Figure 6 are widely used in the field of protein folding to kinetically identify unfolding and refolding intermediates and to characterize the transition state of folding.[30] Conventionally, the apparent folding rates are determined by stopped-flow methods under fluorescence or CD detection for fast folding events with rates above 1 s^{-1} and by manual mixing for slower reactions. Fluorescence probes (Trp and Tyr residues for intrinsic protein fluorescence) monitor the folding reactions locally, whereas CD spectroscopy follows the formation and decay of secondary structure elements. The results of this study present an NMR based method to determine Chevron plots of folding on a residue-by-residue basis. It facilitates the equilibrium conversion between the native and unfolded state, which is also employed by dynamic NMR. For CspB, a 1D ^{1}H line shape analysis of the His29 H$^\epsilon$1 resonance in a urea induced unfolding transition revealed 1460 ± 370 s^{-1} for $k_f^{H_2O}$ and 16 ± 3 s^{-1} for $k_u^{H_2O}$ at 0 M urea as well as 0.9 for the Tanford factor.[11] The substantial uncertainties and deviation from the fluorescence data results mainly from the extrapolation to 0 M urea because dynamic NMR with CspB was only possible between 3 and 5.5 M urea. Also, the experiments were carried

out in D_2O, which might stabilize the protein. The six presented chevron plots in Figure 6 average to 1002 ± 157 s^{-1} for k_{ex} at 0 M urea and 32 ± 14 s^{-1} at 6.4 M urea, which is very close to 1070 ± 20 s^{-1} and 35 ± 7 s^{-1} derived from the stopped-flow fluorescence data. First, it is noteworthy that folding rates from equilibrium and kinetic studies are compared. Second, that the folding rates derived between 0 and 4.2 M urea were determined from cross-peaks of the native state whereas corresponding cross-peaks of the unfolded state were exploited between 5.3 and 6.4 M urea. Third, that the linear extrapolation carried out between 0.6 and 0 M urea in the chevron plot determined by stopped-flow fluorescence was valid. Therefore, the existence of a so far undetected kinetic folding intermediate under strong native conditions can be excluded, because its population would cause a deviation from linearity.[30] This further supports the two-state folding mechanism of CspB and the reliability of both methods.

The NMR derived chevron plots from Val6, Phe15, Ala32, Ala46, Gly54, and Gly57 presented here extend the characterization of the transition state of folding for CspB from the two local probes (Trp 8 by fluorescence spectroscopy[2] and His29 by 1D dynamic NMR[11]) from the first antiparallel β-sheet domain of CspB to all structure elements of the protein. All reporters revealed very similar $k_f^{H_2O}$, $k_u^{H_2O}$, and Tanford factors close to 0.9, which indicates the cooperativity of the folding reaction and that the transition state of folding is very homogeneous in its native like solvent accessible surface area. The homo- and heterogeneity of TS is discussed controversially in the protein folding field.[30,39] This includes interpretations of chevron plots from stopped-flow CD and fluorescence data, which deviate at the limbs under strong native or unfolding conditions from linearity. Here either a shift between a native-like and an unfolded-like TS at various urea concentrations is proposed or more likely a urea dependent shift of the Gibbs free energy of the unfolded state and an invariant TS. The presented approach using transverse relaxation NMR will allow to address such questions by providing residue specific folding and unfolding kinetics. Therefore, the mapping of the transition state is feasible at a residue resolution.

Acknowledgment. We thank P. Rösch for NMR time at the Bruker Avance700 in Bayreuth and the SON NMR Large Scale Facility in Utrecht (The Netherlands), which is funded by the "Access to Research Infrastructures" program of the European Union (HPRI-CT-2001-00172) for NMR time at the Bruker Avance750 and Avance600. This research was supported by grants from the Deutsche Forschungsgemeinschaft (Ba 1821/2-1; Ba 1821/3-1) and the INTAS-2001 program.

JA051141+

(39) Oliveberg, M. *Curr. Opin. Struct. Biol.* **2001**, *11*, 94−100.
(40) Koradi, R.; Billeter, M.; Wüthrich, K. *J. Mol. Graph.* **1996**, *14*, 51−55.